Design Proposal for Reducing Actuator Redundancy in Intrinsically Compliant Manipulators

Valerio Salvucci and Takafumi Koseki
Department of Electrical Engineering and Information System, The University of Tokyo
3-7-1 Hongo Bunkyoku Tokyo, Japan Email: valerio@koseki.t.u-tokyo.ac.jp, takafumikoseki@ieee.org

***Abstract*—Variable Stiffness Actuators (VSA) allow for simultaneous position and stiffness control of a joint by the use of two actuators, therefore they are used in the design of intrinsically compliant manipulators. Generally, for a manipulator with n joints n VSAs are used, resulting in 2n actuators. In this work, we propose the design of a two-link intrinsically compliant manipulator using only three actuators (instead than four): one Series Elastic Actuator (SEA) in a mono-articular configuration, and a VSA based on two antagonistic actuators in biarticular (actuators producing simultaneous torque about both joints) configuration. The proposed actuation structure reduces the amount of actuators, while increasing the isotropy of the end effector force (in all the workspace), and end effector stiffness isotropy when the arm extends. Therefore the proposed structure based on monoarticular SEA and biarticular VSA is suitable for light and compliant manipulation, as for example robotic hands, arms and legs.**

I. Introduction

In human-robot interaction, as well for robots operating in presence of humans, passive compliance is fundamental to guarantee safety [1]. A widely known approach to achieve passive compliance is through the use of elastic elements between the actuator and the joint, namely Series Elastic Actuators (SEAs) [2]. A limit of SEAs is that the compliance can not be varied without the use of feedback control as it depends on the mechanical characteristic of the elastic elements, which is constant [3]. In order to overcome the bandwidth limitations of feedback control, while at the same time allowing for passive compliance regulation, Variable Stiffness Actuators (VSAs) are rising interest. VSAs allow for simultaneous position and stiffness control of a joint by the use of two actuators, therefore they are used in the design of intrinsically compliant manipulators [4]. Generally, for a manipulator with n links n VSAs are used, resulting in $2n$ actuators [5], [6], [7], [8], [9], [10], [11], [12], [13].

In order to overcome many limitation of conventional actuation structure, biarticular actuators have been proposed due to the numerous advantages they yield. Biarticular actuators dramatically increase the range of end effector impedance which can be achieved without feedback [14], increasing the capability of path tracking and disturbance rejection [15], [16], allowing for precise output force control [17], and improving balance control for legged robots without force sensors [18].

Maximum output force at the end effector results in a higher isotropy when biarticular actuators are present [19], [20]. Biarticular actuators transfer mechanical energy from proximal to distal joints [21]. A number of robots have been realized using biarticular actuators, by means of pneumatic actuators [22], and motors with transmissions systems based on pulleys [23], planetary gears [24], wires [25], and passive springs [26]. In [12] a robot finger with VSAs and biarticular actuation structure is proposed. However, is is designed using two VSAs, therefore four actuators.

In order to reduce the number of actuators and the design complexity of intrinsically compliant manipulators, an actuation structure combining SEA in monoarticular configuration and VSA in biarticular configuration is proposed for a two-link intrinsically compliant manipulator. A comparison with the conventional structure using four actuators is carried on.

In Section II, the proposed actuation structure is described together with the modeling. In Section III, the analysis method used to compare the resulting end effector force and stiffness of the proposed and the conventional actuation structure is illustrated. The results are shown in Section IV, and discussed in Section V. Finally, the advantages of the proposed actuation structure are summarized in Section VI.

II. Proposed structure with reduced actuator redundancy

A. Structure

In Fig. 1 the conventional and proposed actuation structures for a two-link intrinsically compliant robot arm are shown.

As a representative example of an intrinsically compliant manipulator actuated by VSAs, a two-link planar manipulator with two VSAs is shown in Fig. 1(a): consists of four monoarticular ($4m$) actuators, arranged in antagonistic configuration and in series to non-linear spring.

The proposed structure ($1m2b$ in Fig. 1(b)), consists of three actuators: one Series Elastic Actuator (SEA) coupled to joint 1 by two linear springs in monoarticular configuration ($1m$), and a VSA made of two biarticular actuators ($2b$) producing torque about both joints by means of two non-linear springs connected to two free pulleys about joint 1 and to two pulleys rotating about joint 2 and fixed on link 2.

B. Modeling

Given the reference system in Fig. 1(a), the spring displacements between joints and respective actuator for the $4m$

978-1-4799-2722-7/13/$31.00 ©2013 IEEE

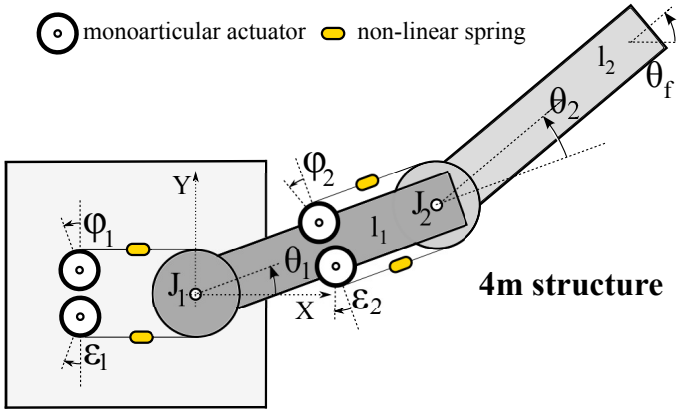

(a) Four mono-articular actuators ($4m$)

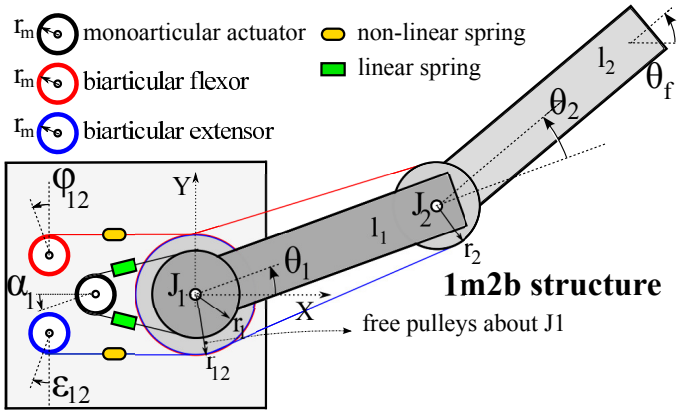

(b) One mono- and two bi-articular actuators ($1m2b$)

Fig. 1. Two-link intrinsically compliant manipulators: conventional and proposed structures

structure are:

$$\Delta l_{\phi 1} = \phi_1 r_m - r_1 \theta_1 \quad (1)$$
$$\Delta l_{\varepsilon 1} = \varepsilon_1 r_m + r_1 \theta_1 \quad (2)$$
$$\Delta l_{\phi 2} = \phi_2 r_m - r_2 \theta_2 \quad (3)$$
$$\Delta l_{\varepsilon 2} = \varepsilon_2 r_m + r_2 \theta_2 \quad (4)$$

where ϕi and εi are respectively the flexor and extensor monoarticular actuator angle displacements in radiant, $\boldsymbol{\theta} = [\theta_1, \theta_2]^{\mathrm{T}}$ is the joint angle position, r_m is the radius of the motor pulleys, and r_1 and r_2 are the radii of pulleys at joint 1 and 2, respectively.

The force-displacement characteristic of the springs is of quadratic form, therefore the resulting forces $f_{(\phi i, \varepsilon i)}$ are:

$$f_{\phi 1} = k_2 \Delta l_{\phi 1}^2 + k_1 \Delta l_{\phi 1} + k_0 \quad (5)$$
$$f_{\varepsilon 1} = k_2 \Delta l_{\varepsilon 1}^2 + k_1 \Delta l_{\varepsilon 1} + k_0 \quad (6)$$
$$f_{\phi 2} = k_2 \Delta l_{\phi 2}^2 + k_1 \Delta l_{\phi 2} + k_0 \quad (7)$$
$$f_{\varepsilon 2} = k_2 \Delta l_{\varepsilon 2}^2 + k_1 \Delta l_{\varepsilon 2} + k_0 \quad (8)$$

The resulting joint torque ($\boldsymbol{T}^{4m}$) is:

$$\boldsymbol{T}^{4m} = \begin{bmatrix} T_1^{4m} \\ T_2^{4m} \end{bmatrix} = \begin{bmatrix} \tau_{\mu 1} \\ \tau_{\mu 2} \end{bmatrix} = \begin{bmatrix} r_1(f_{\phi 1} - f_{\varepsilon 1}) \\ r_2(f_{\phi 2} - f_{\varepsilon 2}) \end{bmatrix} = \quad (9)$$
$$= \begin{bmatrix} r_1(k_2 r_m(\phi_1 + \varepsilon_1) + k_1)(r_m(\phi_1 - \varepsilon_1) - 2r_1\theta_1) \\ r_1(k_2 r_m(\phi_2 + \varepsilon_2) + k_1)(r_m(\phi_2 - \varepsilon_2) - 2r_2\theta_2) \end{bmatrix}$$

where $\tau_{\mu i}$ is the torque resulting at joint i produced by the monoarticular actuator i.

The joint stiffness matrix is:

$$\boldsymbol{K}_{\mathrm{j}}^{4m} = \boldsymbol{J}\boldsymbol{t}_{\boldsymbol{4m}}^{\boldsymbol{T}} \boldsymbol{K}\boldsymbol{t}_{\boldsymbol{4m}} \boldsymbol{J}\boldsymbol{t}_{\boldsymbol{4m}} = \quad (10)$$
$$= \begin{bmatrix} 2r_1^2(k_2 r_m(\phi_1 + \varepsilon_1) + k_1) & 0 \\ 0 & 2r2^2(k_2 r_m(\phi_2 + \varepsilon_2) + k_1) \end{bmatrix}$$

where,

$$\boldsymbol{J}\boldsymbol{t}_{\boldsymbol{4m}}^{\boldsymbol{T}} = \begin{bmatrix} r_1 & -r_1 & 0 & 0 \\ 0 & 0 & r_2 & -r_2 \end{bmatrix} \quad (11)$$

$$\boldsymbol{K}\boldsymbol{t}_{\boldsymbol{4m}} = \begin{bmatrix} 2k_2\Delta l_{\phi 1} + k_1 & 0 \\ 0 & 2k_2\Delta l_{\varepsilon 1} + k_1 \\ 0 & 0 \\ 0 & 0 \\ 0 & 0 \\ 0 & 0 \\ 2k_2\Delta l_{\phi 2} + k_1 & 0 \\ 0 & 2k_2\Delta l_{\varepsilon 2} + k_1 \end{bmatrix} \quad (12)$$

For the $1m2b$ structure, given the reference system in Fig. 1(b), the spring displacements between joints and respective actuator are:

$$\Delta l_{\alpha} = \alpha_1 r_m - r_1 \theta_1 \quad (13)$$
$$\Delta l_{\phi 12} = \phi_{12} r_m - r_{12}\theta_1 - r_2\theta_2 \quad (14)$$
$$\Delta l_{\varepsilon 12} = \varepsilon_{12} r_m + r_{12}\theta_1 + r_2\theta_2 \quad (15)$$

where α_1 is the angle displacement of the monoarticular actuator (which can be positive or negative), $\phi_1 2$ and ε_{12} are respectively the flexor and extensor biarticular actuator angle displacements in radiant, r_{12} is the radius of the free pulley about joint 1.

The forces produced by the springs are:

$$f_{\alpha} = k_3 \Delta l_{\alpha} \quad (16)$$
$$f_{\phi 12} = k_2 \Delta l_{\phi 12}^2 + k_1 \Delta l_{\phi 12} + k_0 \quad (17)$$
$$f_{\varepsilon 12} = k_2 \Delta l_{\varepsilon 12}^2 + k_1 \Delta l_{\varepsilon 12} + k_0 \quad (18)$$

where k_3 is the resultant stiffness coefficient of the two linear springs between the monoarticular motor and joint 1. The force f_{α} can be positive or negative as the springs are considered to operate without any lack.

The resulting joint torque ($\boldsymbol{T}^{1m2b}$) is:

$$\boldsymbol{T}^{1m2b} = \begin{bmatrix} T_1^{1m2b} \\ T_2^{1m2b} \end{bmatrix} = \begin{bmatrix} \tau_{\alpha} + \tau_{\beta 1} \\ \tau_{\beta 2} \end{bmatrix} = \quad (19)$$
$$= \begin{bmatrix} r_1 f_{\alpha} + r_{12}(f_{\phi 12} - f_{\varepsilon 12}) \\ r_2(f_{\phi 12} - f_{\varepsilon 12}) \end{bmatrix}$$

TABLE I. PARAMETERS VALUES

$L_1 = L_2$	1 (m)
Pulleys radii $r_m = r_1 = r_2 = r_{12}$	0.1 (m)
k_0, k_1, k_3	$2, -200, 500$ (N/m)
k_2	10^5 (N^2/m^2)
All motors maximum torque ($\tau^{\max}_{\text{motor}}$)	10 (Nm)
Minimum co-contraction force	5 (N)

$$T_1^{1m2b} = (-2k_2(\phi_{12}+\varepsilon_{12})r_{12}r_2r_m - 2k_1r_{12}r_2)\theta_2 + \quad (20)$$
$$+(-2k_2(\phi_{12}+\varepsilon_{12})r_{12}^2r_m - 2k_1r_{12}^2 - k_3r_1^2)\theta_1 +$$
$$+k_2(\phi_{12}^2-\varepsilon_{12}^2)r_{12}r_m^2 + (k_1(\phi_{12}-\varepsilon_{12})r_{12} + k_3\alpha_1r_1)r_m$$
$$T_2^{1m2b} = r_2(k_2r_m(\phi_{12}+\varepsilon_{12}) + k_1) \quad (21)$$
$$(r_m(\phi_{12}-\varepsilon_{12}) - 2(r_2\theta_2 + r_{12}\theta_1))$$

where τ_α is the torque resulting at joint 1 produced by the monoarticular actuator 1, $\tau_{\beta i}$ is the torque resulting at joint i produced by the biarticular actuators.

The resultant joint stiffness matrix is:

$$\boldsymbol{Kj}^{1m2b} = \boldsymbol{Jt}^T_{1m2b}\boldsymbol{Kt}_{1m2b}\boldsymbol{Jt}_{1m2b} = \begin{bmatrix} Kj_{11}^{1m2b} & Kj_{12}^{1m2b} \\ Kj_{21}^{1m2b} & Kj_{22}^{1m2b} \end{bmatrix} \quad (22)$$

where,

$$Kj_{11}^{1m2b} = 2r_{12}^2r_mk_2(\Delta l_{\varepsilon 12} + \Delta l_{\phi 12}) + 2k_1r_{12}^2 + 2k_3r_1^2 \quad (23)$$
$$Kj_{12}^{1m2b} = Kj_{21}^{1m2b} = 2r_{12}r_2\left(k_2r_m(\Delta l_{\varepsilon 12} + \Delta l_{\phi 12}) + k_1\right) \quad (24)$$
$$Kj_{22}^{1m2b} = 2r_2^2\left(k_2r_m(\Delta l_{\varepsilon 12} + \Delta l_{\phi 12}) + k_1\right) \quad (25)$$

$$\boldsymbol{Jt^T_{1m2b}} = \begin{bmatrix} r_1 & -r_1 & r_{12} & -r_{12} \\ 0 & 0 & r_2 & -r_2 \end{bmatrix} \quad (26)$$

$$\boldsymbol{Kt_{1m2b}} = \begin{bmatrix} k_3 & 0 & 0 & 0 \\ 0 & k_3 & 0 & 0 \\ 0 & 0 & 2k_2\Delta l_{\phi 12} + k_1 & 0 \\ 0 & 0 & 0 & 2k_2\Delta l_{\varepsilon 12} + k_1 \end{bmatrix} \quad (27)$$

The stiffness matrix in Cartesian coordinates, $\boldsymbol{K}^{(4m,1m2b)}$, is:

$$\boldsymbol{K}^{(4m,1m2b)} = \left(\boldsymbol{J}^{\mathrm{T}}\right)^{-1}\boldsymbol{K}_{\mathrm{j}}^{(4m,1m2b)}(\boldsymbol{J})^{-1} \quad (28)$$

where $\boldsymbol{J}$ is the robot arm analytical Jacobian matrix:

$$\boldsymbol{J} = \begin{bmatrix} -L_1\sin(\theta_1) - L_2\sin(\theta_1+\theta_2) & -L_2\sin(\theta_1+\theta_2) \\ L_1\cos(\theta_1) + L_2\cos(\theta_1+\theta_2) & L_2\cos(\theta_1+\theta_2) \end{bmatrix} \quad (29)$$

The parameters of the two-link arm and the two actuation structures are shown in Tab. I. The parameters for the quadratic springs have been chosen as an approximation of the values of the quadratic springs used in [6]. As for the linear springs, a value of the same order of magnitude of the linear coefficient of the quadratic springs (k_1) available on the market has been chosen. Every pulley radii, as well every maximum motor torque, have been chosen with same value, therefore all the maximum joint actuator torques in which a non-linear spring is present is same ($\tau^{\max}_{(\mu 1,\mu 2,\beta 1,\beta 2)} = 9.5$ Nm) due to the minimum co-contraction force set to 5 N, while the monoarticular actuator with linear springs (SEA) has $\tau_\alpha^{\max} = 10$ Nm.

III. ANALYSIS METHOD

The $4m$ and $1m2b$ structures are compared in terms of both end effector force and stiffness. As for the end effector force the vector of maximum output force, $\boldsymbol{F}^{\max}$, in condition of minimum stiffness is calculated using an iterative algorithms as in [20]. Then, the force in the maximum output force space with minimum magnitude $\boldsymbol{FSmin}$ equal to

$$\boldsymbol{FSmin} = \boldsymbol{F}^{\max} \text{ s.t. } |\boldsymbol{F}^{\max}| \text{ is minimum for } \theta^f \in (0, 2\pi),$$

where θ^f is the end effector output force direction, is calculated, and its magnitude ($|\boldsymbol{FSmin}|$) is evaluated as measure of the isotropy of the maximum output force.

The end effector stiffness isotropy is compared using the condition number (cn) of minimum and maximum Cartesian stiffness defined as [27]:

$$cn^{(4m,1m2b)}_{(minsti,maxsti)} = \frac{\max(\lambda(\boldsymbol{K}^{(4m,1m2b)}_{(minsti,maxsti)}))}{\min(\lambda(\boldsymbol{K}^{(4m,1m2b)}_{(minsti,maxsti)}))} \quad (30)$$

where $\lambda(\boldsymbol{K})$ are the eigenvalues of $\boldsymbol{K}$.

The minimum (or maximum) Cartesian stiffness is calculate when the end effector force is null and the antagonistic actuators co-contraction force is minimum 5 N (or maximum 100 N).

IV. RESULTS

A. End effector force

In Fig. 2 the resulting maximum output force for both structures and two arm configurations: extended arm, $\boldsymbol{\theta} = [0, 30^\circ]^{\mathrm{T}}$, and bended arm $\boldsymbol{\theta} = [0, 150^\circ]^{\mathrm{T}}$. The value of $\boldsymbol{FSmin}$ for both structure is also represented by arrows.

The magnitude of $\boldsymbol{FSmin}$ ($|\boldsymbol{FSmin}|$) in respect to θ_2 is shown in Fig. 3. Due to the presence of biarticular actuators, $|\boldsymbol{FSmin}|$ for the $1m2b$ structure is greater (or equal) to the $|\boldsymbol{FSmin}|$ of $4m$ structure. As a result the maximum end effector force presents a higher isotropy. In addition, sue to the fact that $L_1 = L_2 = L$, $|\boldsymbol{FSmin}|$ is constant in all the work space (as long as the arm in not in singular configuration) and equal to 9.5 N as shown in Appendix A.

B. End effector stiffness

In Fig. 4 the resulting minimum and maximum stiffness Cartesian stiffness for both the actuation structure are shown for two arm configurations: extended arm, $\boldsymbol{\theta} = [0, 30^\circ]^{\mathrm{T}}$, and bended arm $\boldsymbol{\theta} = [0, 150^\circ]^{\mathrm{T}}$.

In order to compare the stiffness isotropy, the condition numbers of Cartesian stiffness for both actuation structure is shown in Fig. 5 (miniumum stiffness in Fig. 5(a), and maximum stiffness in Fig. 5(b)).

V. DISCUSSION

On the basis of the design and carried on analysis, it is deduced that by using the proposed actuation structure:

- The number of actuators is reduced from four to three. In addition, the number of necessary non-linear springs is reduced from four to two.

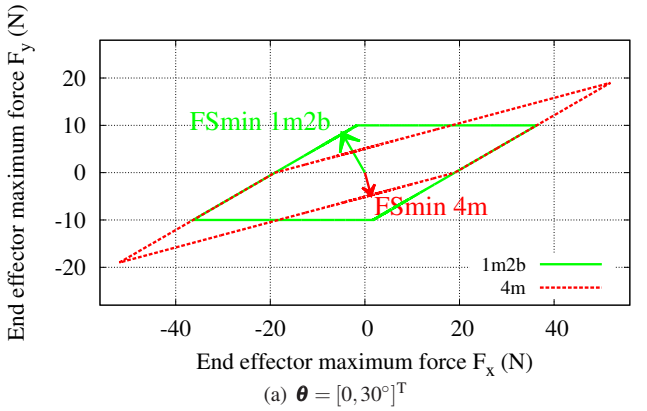

(a) $\boldsymbol{\theta} = [0, 30°]^T$

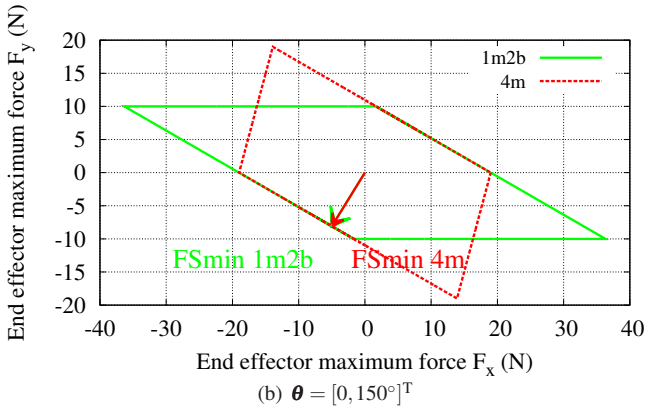

(b) $\boldsymbol{\theta} = [0, 150°]^T$

Fig. 2. Maximum output force space and resulting minimum force ($\boldsymbol{FSmin}$) for both actuation structure

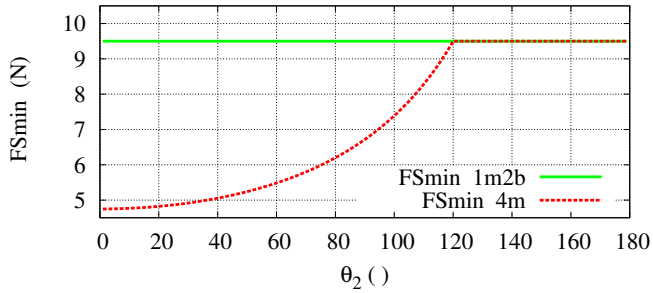

Fig. 3. $|\boldsymbol{FSmin}|$ for $4m$ and $1m2b$ structures in respect to θ_2. $\boldsymbol{\theta} = [0, (1-179)°]^T$

- The equilibrium position and the end effector stiffness can be independently controlled.
- The equilibrium position and the stiffness of each joint can not be independently controlled.
- The isotropy of the maximum end effector force is higher (or equal) in all the work space. In addition, the minimum force at the end effector is independent from manipulator configuration (as long it is not singular). As a consequence, the actuation system design of robot arms is furthermore simplified.
- Both minimum and maximum Cartesian stiffness presents a lower isotropy when the arm is bended, while a higher isotropy when the arm is extended.

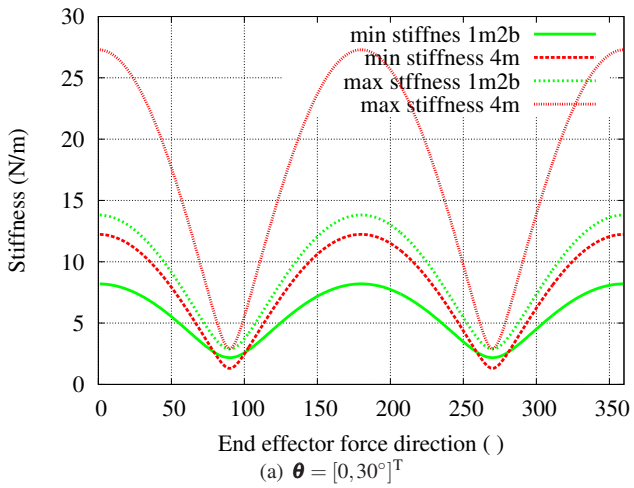

(a) $\boldsymbol{\theta} = [0, 30°]^T$

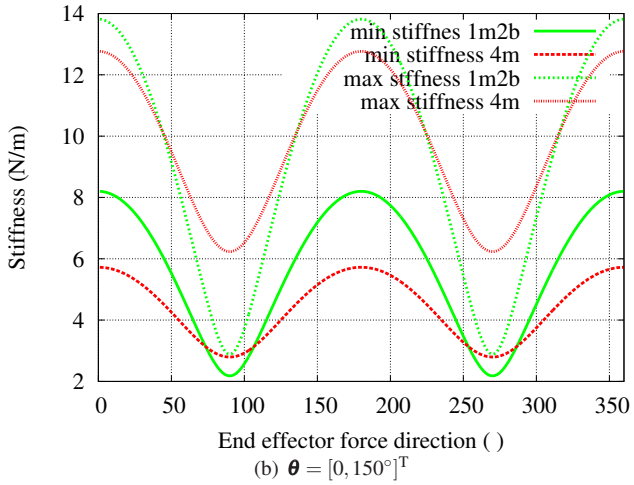

(b) $\boldsymbol{\theta} = [0, 150°]^T$

Fig. 4. Minimum and maximum end effector Cartesian stiffness ($|\boldsymbol{F}^{out}| = 0$)

In Tab. II the general comparison between the $4m$ and $1m2b$ actuation structure is summarized.

The analysis carried on in this work is based on VSAs in antagonistic configuration, i.e. actuators characterized by two actuators in antagonistic configuration coupled with the arm link through non-linear spring. If VSAs with serial configuration (i.e. series combination of actuator, elastic element and joint, with a second actuator varying the joint stiffness by changing the preload on the elastic elements), in the proposed structure the VSA would be in biarticular configuration, and the SEA in monoarticular configuration.

VI. Conclusions

In this work, we propose a new actuation structure combining Series Elastic Actuators in monoarticular configuration and Variable Stiffness Actuators in biarticular configuration. The proposed structure has the advantage of reducing the number of actuators (from four to three), allowing however simultaneous control of position and stiffness at the end effector.

The end effector maximum force present a higher isotropy thanks to the biarticular actuation structure. The end effector

TABLE II. GENERAL COMPARISON BETWEEN THE $4m$ AND $1m2b$ ACTUATION STRUCTURE

	$4m$	$1m2b$
Number of actuators	4	3
Independent position-stiffness control of every joint	possible	not possible
Independent position-stiffness control of end effector	possible	
Maximum force isotropy	lower	higher
Minimum end effector stiffness isotropy	higher when arm bended	higher when arm stretched
Maximum end effector stiffness isotropy	higher when arm bended	higher when arm stretched

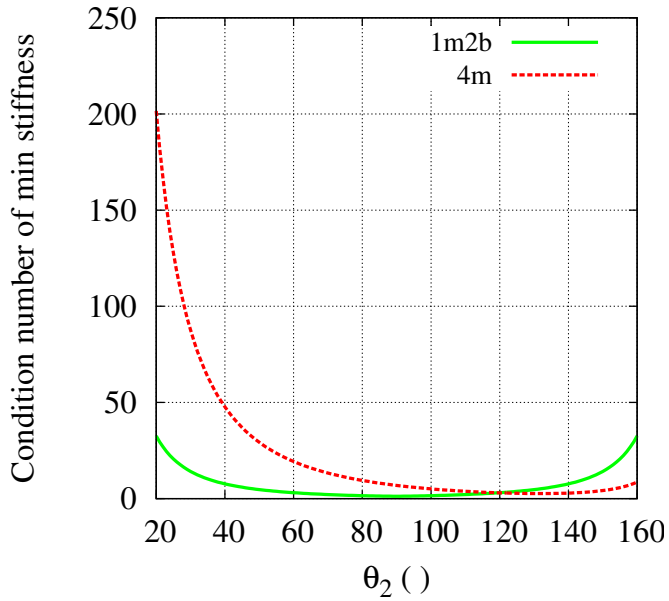

(a) Minimum Cartesian stiffness

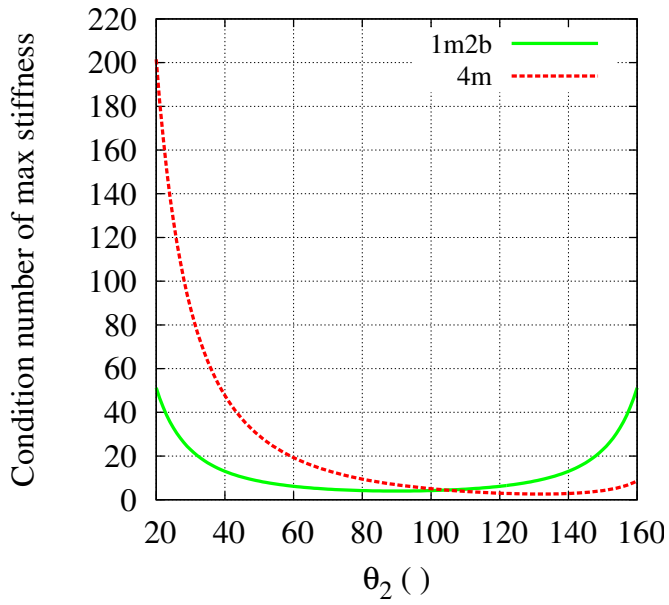

(b) Maximum Cartesian stiffness

Fig. 5. Condition numbers of Cartesian stiffness in respect to θ_2

stiffness is more isotropic when the robot arm stretches. This is an advantage as stretched position of the arm are more challenging to control due to the increasing non linearities of the jacobian.

Therefore, the proposed structure is suitable for intrinsically compliant manipulators requiring low weight and operating in presence of humans, as for example robotic fingers, arms and legs.

Future works include the experimental validation of the proposed design, as well the analysis to robot arm with more than two links.

APPENDIX A
PROOF OF CONSTANT $|FSmin|$ IN THE ENTIRE WORKSPACE

Given the fact that θ_1 merely rotates the maximum output force space, in the following $\theta_1 = 0$. Given $\theta_1 = 0$, and $L_1 = L_2 = L$, the analytical Jacobian $\boldsymbol{J}_0$ is:

$$\boldsymbol{J}_0 = \begin{bmatrix} -L\sin(\theta_2) & -L\sin(\theta_2) \\ L + L\cos(\theta_2) & L\cos(\theta_2) \end{bmatrix} \tag{31}$$

The magnitude of the force at the end effector $|\boldsymbol{F}|$ is:

$$|\boldsymbol{F}| = \sqrt{F_x^2 + F_y^2} = \tag{32}$$

$$= \frac{\sqrt{\tau_\alpha^2 - 2\cos(\theta_2)\tau_\alpha\tau_\beta + \tau_\beta^2}}{L|\sin\theta_2|} \tag{33}$$

where

$$\boldsymbol{F} = \begin{bmatrix} F_x \\ F_y \end{bmatrix} = \left(\boldsymbol{J}_0^{\mathrm{T}}\right)^{-1} \boldsymbol{T}^{1m2b} \tag{34}$$

and τ_α is the torque resulting at joint 1 produced by the monoarticular actuator 1, $\tau_\beta = \tau_{\beta 1} = \tau_{\beta 2}$ is the torque resulting at joint i produced by the biarticular actuators.

The derivatives of $|\boldsymbol{F}|$ with respect to τ_α and τ_β are:

$$\frac{\delta|\boldsymbol{F}|}{\delta\tau_\alpha} = \frac{\tau_\alpha - \tau_\beta\cos(\theta_2)}{L|\sin(\theta_2)|\sqrt{{\tau_\alpha}^2 - 2\tau_\beta\cos(\theta_2)\tau_\alpha + {\tau_\beta}^2}} \tag{35}$$

$$\frac{\delta|\boldsymbol{F}|}{\delta\tau_\beta} = \frac{\cos(\theta_2)\tau_\alpha - \tau_\beta}{L|\sin(\theta_2)|\sqrt{{\tau_\alpha}^2 - 2\tau_\beta\cos(\theta_2)\tau_\alpha + {\tau_\beta}^2}} \tag{36}$$

The points in which $\tau_\alpha = \tau_\beta cos(\theta_2)$ and $\tau_\beta = \tau_\alpha cos(\theta_2)$ are minimum or maximum of the function $|\boldsymbol{F}|$.

The Hessian matrix of $|\boldsymbol{F}|$ in respect to τ_α and τ_β is:

$$\boldsymbol{H}^{1m2b} = \begin{bmatrix} H_{11}^{1m2b} & H_{12}^{1m2b} \\ H_{21}^{1m2b} & H_{22}^{1m2b} \end{bmatrix} = \begin{bmatrix} \frac{\delta^2|\boldsymbol{F}|}{\delta\tau_\alpha^2} & \frac{\delta^2|\boldsymbol{F}|}{\delta\tau_\alpha\tau_\beta} \\ \frac{\delta^2|\boldsymbol{F}|}{\delta\tau_\beta\tau_\alpha} & \frac{\delta^2|\boldsymbol{F}|}{\delta\tau_\beta^2} \end{bmatrix}$$

where

$$H_{11}^{1m2b} = -\frac{{\tau_\beta}^2\left(\cos\left(\theta_2\right)-1\right)\left(\cos\left(\theta_2\right)+1\right)}{L\left|\sin\left(\theta_2\right)\right|\left({\tau_\alpha}^2-2\tau_\alpha\tau_\beta\cos\left(\theta_2\right)+{\tau_\beta}^2\right)^{\frac{3}{2}}} \quad (37)$$

$$H_{12}^{1m2b} = \frac{\tau_\beta\left(\cos\left(\theta_2\right)-1\right)\left(\cos\left(\theta_2\right)+1\right)\tau_\alpha}{L\left|\sin\left(\theta_2\right)\right|\left({\tau_\alpha}^2-2\tau_\alpha\tau_\beta\cos\left(\theta_2\right)+{\tau_\beta}^2\right)^{\frac{3}{2}}} \quad (38)$$

$$H_{21}^{1m2b} = H_{12}^{1m2b} \quad (39)$$

$$H_{22}^{1m2b} = -\frac{\left(\cos\left(\theta_2\right)-1\right)\left(\cos\left(\theta_2\right)+1\right){\tau_\alpha}^2}{L\left|\sin\left(\theta_2\right)\right|\left({\tau_\alpha}^2-2\tau_\alpha\tau_\beta\cos\left(\theta_2\right)+{\tau_\beta}^2\right)^{\frac{3}{2}}} \quad (40)$$

The determinant of $\boldsymbol{H}^{1m2b}$ is null. However, it is positive semi-definite as its eigenvalues are all non-negative:

$$\lambda(\boldsymbol{H}^{1m2b}) = \begin{bmatrix} \frac{\left(1-\cos(\theta_2)^2\right)\left({\tau_\alpha}^2+{\tau_\beta}^2\right)}{L\left|\sin(\theta_2)\right|\left({\tau_\alpha}^2-2\tau_\alpha\tau_\beta\cos(\theta_2)+{\tau_\beta}^2\right)^{\frac{3}{2}}} \\ 0 \end{bmatrix}$$

As a consequence, $\tau_\alpha = \tau_\beta cos(\theta_2)$ and $\tau_\beta = \tau_\alpha cos(\theta_2)$ are two minimum points of $|\boldsymbol{F}|$.

The value of $|\boldsymbol{F}|$ in these two points is $\frac{|\tau_\beta|}{L}$ and $\frac{|\tau_\alpha|}{L}$, respectively. Such values do not depend on θ_2, as long as the robot arm is not in a singular configuration.

Therefore, $|\boldsymbol{FSmin}|$ (the minimum value of $|\boldsymbol{F}^{\max}|$) is:

$$|\boldsymbol{FSmin}| = \min(\frac{\tau_\alpha^{\max}}{L}, \frac{\tau_\beta^{\max}}{L}) = \min(\frac{10}{1}, \frac{9.5}{1}) = 9.5 \quad (41)$$

REFERENCES

[1] A. Bicchi, S. Rizzini, and G. Tonietti, "Compliant design for intrinsic safety: general issues and preliminary design," in *2001 IEEE/RSJ International Conference on Intelligent Robots and Systems, 2001. Proceedings*, vol. 4, 2001, pp. 1864–1869 vol.4.

[2] G. A. Pratt and M. M. Williamson, "Series elastic actuators," in *Intelligent Robots and Systems 95.'Human Robot Interaction and Cooperative Robots', Proceedings. 1995 IEEE/RSJ International Conference on*, vol. 1, 1995, pp. 399–406.

[3] C. English and D. Russell, "Mechanics and stiffness limitations of a variable stiffness actuator for use in prosthetic limbs," *Mechanism and Machine Theory*, vol. 34, no. 1, pp. 7–25, Jan. 1999.

[4] R. Ham, T. Sugar, B. Vanderborght, K. Hollander, and D. Lefeber, "Compliant actuator designs," *IEEE Robotics Automation Magazine*, vol. 16, no. 3, pp. 81–94, 2009.

[5] K. Koganezawa, T. Inaba, and T. Nakazawa, "Stiffness and angle control of antagonistially driven joint," in *The First IEEE/RAS-EMBS International Conference on Biomedical Robotics and Biomechatronics, 2006. BioRob 2006*, 2006, pp. 1007–1013.

[6] S. Migliore, E. Brown, and S. DeWeerth, "Biologically inspired joint stiffness control," in *International Conference on Robotics and Automation (ICRA)*, 2005, pp. 4508–4513.

[7] J. Hurst, J. Chestnutt, and A. Rizzi, "The actuator with mechanically adjustable series compliance," *IEEE Transactions on Robotics*, vol. 26, no. 4, pp. 597–606, 2010.

[8] I. Thorson, M. Svinin, S. Hosoe, F. Asano, and K. Taji, "Design considerations for a variable stiffness actuator in a robot that walks and runs," in *Proceedings of the Robotics and Mechatronics Conference (RoboMec)*, 2007, p. 14.

[9] R. V. Ham, M. V. Damme, B. Verrelst, B. Vanderborght, and D. Lefeber, "MACCEPA, the mechanically adjustable compliance and controllable equilibrium position actuator: A 3DOF joint with two independent compliances," *International Applied Mechanics*, vol. 43, no. 4, pp. 467–474, Apr. 2007.

[10] S. Wolf and G. Hirzinger, "A new variable stiffness design: Matching requirements of the next robot generation," in *IEEE International Conference on Robotics and Automation, 2008. (ICRA) 2008*, 2008, pp. 1741–1746.

[11] N. G. Tsagarakis, M. Laffranchi, B. Vanderborght, and D. Caldwell, "A compact soft actuator unit for small scale human friendly robots," in *International Conference on Robotics and Automation (ICRA)*, 2009, pp. 4356–4362.

[12] M. Chalon, T. Wimbock, and G. Hirzinger, "Torque and workspace analysis for flexible tendon driven mechanisms," in *International Conference on Robotics and Automation (ICRA)*, 2010, pp. 1175–1181.

[13] G. Palli, C. Melchiorri, T. Wimbock, M. Grebenstein, and G. Hirzinger, "Feedback linearization and simultaneous stiffness-position control of robots with antagonistic actuated joints," in *International Conference on Robotics and Automation (ICRA)*, 2007, pp. 4367–4372.

[14] N. Hogan, "Impedance control: An approach to manipulation: Part III—Applications," *Journal of Dynamic Systems, Measurement, and Control*, vol. 107, no. 1, pp. 17–24, Mar. 1985.

[15] V. Salvucci, S. Oh, Y. Hori, and Y. Kimura, "Disturbance rejection improvement in non-redundant robot arms using bi-articular actuators," in *Intern. Symp. on Industrial Electronics (ISIE)*, 2011, pp. 2159–2164.

[16] T. Horita, P. V. Komi, C. Nicol, and H. Kyrlinen, "Interaction between pre-landing activities and stiffness regulation of the knee joint musculoskeletal system in the drop jump: implications to performance," *European Jour. of Appl. Physiology*, vol. 88, no. 1-2, pp. 76–84, 2002.

[17] V. Salvucci, Y. Kimura, S. Oh, and Y. Hori, "Non-linear phase different control for precise output force of bi-articularly actuated manipulators," *Advanced Robotics*, vol. 27, no. 2, pp. 109–120, 2013.

[18] S. Oh, Y. Kimura, and Y. Hori, "Reaction force control of robot manipulator based on biarticular muscle viscoelasticity control," in *Advanced Intelligent Mechatronics (AIM)*, 2010, pp. 1105–1110.

[19] V. Salvucci, Y. Kimura, S. Oh, and Y. Hori, "Force maximization of biarticularly actuated manipulators using infinity norm," *IEEE/ASME Transactions on Mechatronics*, vol. 18, no. 3, pp. 1080–1089, Jun. 2013.

[20] V. Salvucci, Y. Kimura, S. Oh, T. Koseki, and Y. Hori, "Comparing approaches for actuator redundancy resolution in bi-articularly actuated robot arms," *Mechatronics, IEEE/ASME Transactions on*, May 2013.

[21] G. J. Van Ingen Schenau, "From rotation to translation: Constraints on multi-joint movements and the unique action of bi-articular muscles," *Human Movement Science*, vol. 8, no. 4, pp. 301–337, Aug. 1989.

[22] R. Niiyama, S. Nishikawa, and Y. Kuniyoshi, "Athlete robot with applied human muscle activation patterns for bipedal running," in *International Conference on Humanoid Robots*, 2010, pp. 498–503.

[23] T. Tsuji, "A model of antagonistic triarticular muscle mechanism for lancelet robot," in *2010 11th IEEE International Workshop on Advanced Motion Control*. IEEE, Mar. 2010, pp. 496–501.

[24] Y. Kimura, S. Oh, and Y. Hori, "Novel robot arm with bi-articular driving system using a planetary gear system and disturbance observer," in *International Workshop on Advanced Motion Control (AIM)*, 2010, pp. 296–301.

[25] V. Salvucci, Y. Kimura, S. Oh, and Y. Hori, "BiWi: bi-articularly actuated and wire driven robot arm," in *IEEE International Conference on Mechatronics (ICM)*, Apr. 2011, pp. 827–832.

[26] A. Seyfarth, F. Iida, R. Tausch, M. Stelzer, O. von Stryk, and A. Karguth, "Towards bipedal jogging as a natural result of optimizing walking speed for passively compliant Three-Segmented legs," *Intern. Journal of Robotics Research*, vol. 28, no. 2, pp. 257 –265, 2009.

[27] N. Kashiri, N. G. Tsagarakis, M. Laffranchi, and D. G. Caldwell, "On the stiffness design of intrinsic compliant manipulators," in *IEEE Advanced Intelligent Mechatronics (AIM)*, 2013.